Auxiliary Material for paper 2007GLXXXXXX
Aura Microwave Limb Sounder Upper Tropospheric and Lower Stratospheric H_2O and RHi Validation

W. G. Read, A. Lambert, J. Bacmeister[1], R. E. Cofield, L. E. Christensen, D. T. Cuddy, W. H. Daffer, B. J. Drouin, E. Fetzer, L. Froidevaux, R. Fuller, R. Herman, R. F. Jarnot, J. H. Jiang, Y. B. Jiang, K. Kelly[2], B. W. Knosp, L. J. Kovalenko, N. J. Livesey, H.-C. Liu[1], G. L. Manney, H. M. Pickett, H. C. Pumphrey[3], K. H. Rosenlof[2], X. Sabounchi, M. L. Santee, M. J. Schwartz, W. V. Snyder, P. C. Stek, H. Su, L. L. Takacs[1], R. P. Thurstans, H. Vömel[4], P. A. Wagner, J. W. Waters, C. R. Webster, E. M. Weinstock[4], D. L. Wu

Jet Propulsion Laboratory, California Institute of Technology, Pasadena, CA.

J. Bacmeister, H.-C. Liu, L. L. Takacs

Global Modeling and Assimilation Office, NASA Goddard Space Flight Center, 8800 Greenbelt Road, Greenbelt, MD, 20771-0001

K. Kelly, K. H. Rosenlof

NOAA ESRL Chemical Sciences Division, Mail Stop R/CSD-6, 325 Broadway, Boulder, CO 80305. (Karen.H.Rosenlof@noaa.gov)

H. C. Pumphrey

Department of Meteorology, University of Edinburgh

E. M. Weinstock

Department of Chemistry and Chemical Biology, Harvard University

H. Vömel

Cooperative Institute for Research in Environmental Sciences, University of Colorado

1. Optically thick radiance theory

We present here a simplified theory for the optically thick radiance as it applies to relative humidity measurements. Nadir sounding remote sensors use this technique in their humidity measurements. This approach is used for the middle tropospheric humidity constraint in v2.2 MLS. The theory has been presented elsewhere [*Soden and Bretherton*, 1993] but has been modified for the monochromatic case suitable for instruments with high spectral resolution with an emphasis on the sensitivity of relative humidity to instrumental systematic errors. Taking advantage that temperature in the troposphere monotonically decreases with height, it is advantageous to use temperature as a vertical coordinate in the radiative transfer equation,

$$I_B = \int_{T_s}^{0} \tau(B)\,\mathrm{d}B, \tag{1}$$

where I_B is the radiance and B is the Planck blackbody function and T_s is the surface temperature. In the Rayleigh-Jeans limit $I_B = T_B$ and $B = T$, where T is temperature. The transmission integral is

$$\tau = \exp\left[-\int_{T}^{0} \alpha(t)\,\frac{\mathrm{d}s}{\mathrm{d}R}\frac{\mathrm{d}R}{\mathrm{d}T}\mathrm{d}t\right], \tag{2}$$

where α is the absorption coefficient, s is the line-of-sight distance from the path tangent relative to the center of the Earth (See Figure 2), and R is the distance from the center of Earth to s. The absorption coefficient is $f\beta$, where f is the H_2O volume mixing ratio and β is the H_2O cross section. The cross section, mixing ratio, relative humidity, Planck, hydrostatic, path length derivative with respect to height and temperature functions are represented as:

$$\begin{aligned}
\beta &= VP^a \exp(-nX), \\
f &= \frac{r\mathrm{es}_o}{P} \exp(\lambda X), \\
r &= r_o \exp(\gamma X), \\
B &= B_o \exp(AX), \\
P &= P_o \exp\left(\frac{H}{\wp} X\right), \\
\frac{\mathrm{d}s}{\mathrm{d}R} &= \frac{\mathrm{d}s}{\mathrm{d}R_o} \exp(MX), \\
T &= T_o + \wp(R - R_o),
\end{aligned} \tag{3}$$

where $X = (T - T_o)/T_o$, T_o is the temperature at a reference height, R_o, P is path pressure, V is the frequency and temperature dependent proportionality constant for the cross section evaluated at T_o, n is the temperature dependence of V, a is the pressure dependence of the cross section which varies from 0 on line center to 2 on line wing, es_o is the H_2O saturation vapor pressure at the reference height, λ is the dependence of the H_2O saturation vapor pressure on temperature, r is the relative humidity, r_o is the relative humidity at the reference height, γ is the vertical gradient in the relative humidity profile, B_o is the Planck function at the reference height, $A = h\nu / \left\{ kT_o \left[1 - \exp\left(-\frac{h\nu}{kT_o} \right) \right] \right\}$, P_o is the pressure at the reference height, $\wp$ is the temperature lapse rate, $\frac{\mathrm{d}s}{\mathrm{d}R_o} = \sqrt{R_T / 2(R_o - R_T)}$, and $M = -T_o / [2\wp(R_o - R_T)]$. The reference height, R_o is chosen to be the height of the maximum in the radiance weighting function with respect to r. The path length function is given for a shallow viewing angle relative to the horizon which is appropriate for MLS. This is a poor approximation to the path derivative, but is necessary to achieve an integrable result. It will be shown later that the effect of this approximation is benign in the overall theory. For a typical nadir or cone scanning instrument, $\frac{\mathrm{d}s}{\mathrm{d}R_o} = 1/\cos\phi$ where ϕ is the viewing angle relative to nadir, and $M = 0$. The functions in eq. 3 are inserted into eq. 1 and 2 and evaluated according to *Soden and Bretherton* [1993]. Taking that result and convolving it with a very narrow antenna gives

$$\frac{I_A}{B_o} = \varepsilon \left(\frac{r_o F}{\wp E} \right)^{-A/E} \Gamma\left(1 + \frac{A}{E} \right), \tag{4}$$

where $E = \lambda + \gamma - n + (a-1)H/\wp + M$, $F = \mathrm{es}_o V P_o^{a-1} \frac{\mathrm{d}s}{\mathrm{d}R_o}$, and $\Gamma(x)$ is the gamma function. The poorly approximated path length function whose dependence is M in E varies between 3–6 over integrated values of t where the integrand is large. This is a small contribution to E which is $\sim$30 and therefore the path length approximation is acceptable for studying the behavior and sensitivities of the optically thick radiance model. The antenna convolution adds the antenna transmission term which is a significant systematic error consideration for MLS. Substituting the approximate Planck radiation function for I_A and taking the logarithm of both sides gives

$$T_A = T_o + \frac{T_o}{A} \ln\varepsilon - \frac{T_o}{E} \ln\left(\frac{r_o F}{\wp E} \right) + \frac{T_o}{A} \ln\left[\Gamma\left(1 + \frac{A}{E} \right) \right] \tag{5}$$

showing the well known proportionality between T_A and the logarithm of relative humidity [*Soden and Bretherton*, 1993]. The result here differs from that in *Soden and Bretherton* [1993] because they present the solution integrated over multiple unresolved H_2O lines. Vertical weighting functions of eq. 1 are twice as broad as those from limb viewing but the horizontal resolution is very good (e.g. Aqua AIRS is 9 km). It is worth noting that in the shallow viewing angle relative to the horizon which is appropriate for the MLS scan, produces vertical weighting functions that are only 30% broader than for the optically thin limb viewing condition. Sensitivity to humidity is lost when the vertical temperature gradient vanishes. Therefore nadir sounding techniques are not effective for measuring H_2O near the tropopause.

Figure 1 shows a scatter plot of 383 hPa relative humidity versus band 5 channel 1 radiance at the lowest MLS pointing between 30°S–30°N. The radiances were calculated using the full MLS measurement forward model and do not use the approximations needed to derive eq. 5. The atmosphere is opaque at the lowest MLS pointing. The peak of the radiance weighting function with respect to RHi is near 383 hPa. The linear relation between logarithm of relative humidity and radiance is evident as predicted by eq. 5. This capability prompted us to use this approach for constraining H_2O concentrations below 316 hPa. Thick clouds depress the radiance relative to its clear sky value. This causes retrieved RHi to exceed 100%. All RHi exceeding 110% are set to 110% for the cloud analysis routines [*Wu et al., This Issue*].

Taking the derivative of eq. 5 and rearranging gives the fractional sensitivity of relative humidity to other parameters,

$$\frac{\mathrm{d}r}{r} \approx -E\frac{\mathrm{d}T_A}{T_o} + \frac{E}{A}\frac{\mathrm{d}\varepsilon}{\varepsilon} + \frac{\mathrm{d}\wp}{\wp} - \frac{\mathrm{d}V}{V} + w_b \text{ term}, \tag{6}$$

where small contributing terms are neglected.

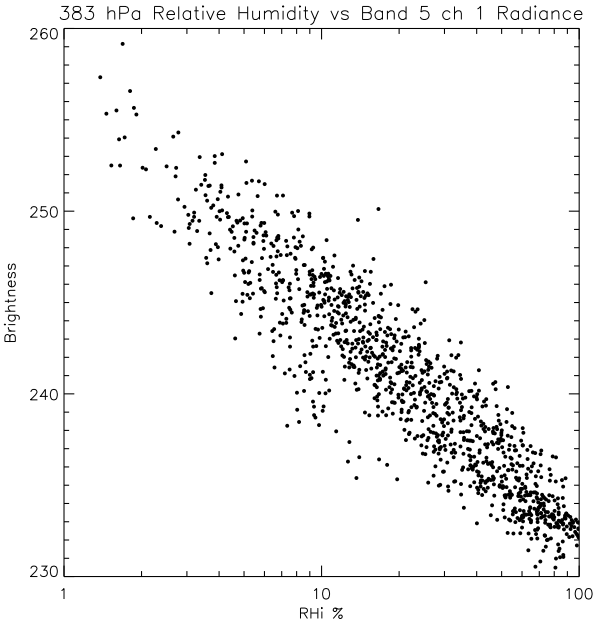

Figure 1. Scatter plot of band 5 channel 1 radiance versus 383 hPa RHi.

The constant $E \approx 30$ is dominated by the temperature sensitivity of the saturation pressure to temperature. Eq. 6, shows that E significantly amplifies radiance scaling errors arising from instrument noise, gain uncertainties, forward model errors, and transmission errors. The blackbody constant, $A = 1$ for microwave and therefore a 1% error in any of these sources is a 30% relative humidity error.

2. Optically thin limb radiance theory

A simple analytical expression for limb radiances is presented here to provide insight into the limb viewing measurement system and is used for some of the systematic error analysis. The full limb viewing measurement model is given in *Read et al.* [2006]. Figure 2 shows the limb viewing geometry. A limb ray is characterized by its tangent height R_T and a path length s. The radiance assuming the Rayleigh-Jeans approximation to the Planck function is given by

$$T_B = T \int_{-\infty}^{\infty} \alpha(s)\,\tau(s)\,\mathrm{d}s, \tag{7}$$

where T is temperature assumed isothermal, α is the absorption coefficient and τ is the atmospheric transmission. A small nearly spectrally flat cosmic space background contribution is ignored. The path length as a function of path

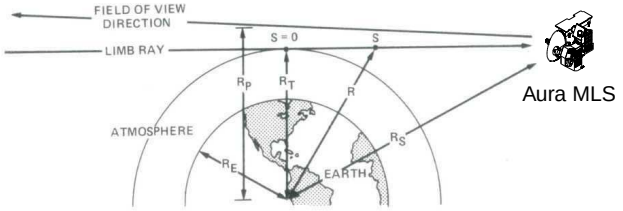

Figure 2. Limb viewing geometry.

height R and tangent height R_T illustrated in Figure 2 is

$$R - R_T \approx \frac{s^2}{2R_T}. \tag{8}$$

The atmospheric transmission is given by

$$\tau(s) = \exp\left[-\int_{-\infty}^{s} \alpha(x)\,\mathrm{d}x\right], \tag{9}$$

where α is the absorption coefficient given by

$$\alpha(s) = f(s)\,\beta(s) \tag{10}$$

where $f(s)$ is the absorbing molecule's mixing ratio and $\beta(s)$ is its cross section. We consider only one absorber in the simple theory. We make use of the following approximate functions,

$$\begin{aligned} \beta &= V\theta^n P^a, \quad \theta = \frac{T_o}{T}, \quad a = \mathrm{d}\ln\beta/\mathrm{d}\ln P, \\ f &= f_T\left(\frac{P}{P_T}\right)^{\gamma}, \\ P &= P_T \exp\left[-\frac{H}{T}(R - R_T)\right], \quad H = \frac{mg}{k}, \end{aligned} \tag{11}$$

where P is path pressure, P_T is limb tangent pressure, V is the frequency and temperature dependent proportionality constant for the cross section evaluated at T_o, n is the temperature dependence of V, a is the pressure dependence of the cross section which varies from 0 on line center to 2 on line wing, γ is the vertical gradient for mixing ratio, m is the mean molecular mass, g is the gravitational acceleration, and k is the Boltzmann constant.

Eqns. 8–11 are combined and substituted into eq. 7 to give

$$T_B = T\alpha_T \int_{-\infty}^{\infty} \exp\left(-C^2 s^2\right) \exp\left\{-\frac{\alpha_T\sqrt{\pi}}{2C}\left[1 + \mathrm{erf}(Cs)\right]\right\} \mathrm{d}s, \tag{12}$$

where $\mathrm{erf}(Cs)$ is the error function, $\alpha_T = V\theta^n f_T P_T^a$ and $C = \sqrt{H(a+\gamma)/(2R_T T)}$. We assume constants a, n, H,

and γ do not vary along s. Eq. 12 is accurate for optical thin and thick situations. For a weak absorbing atmosphere, $\mathrm{erf}(Cs) \approx 2Cs/\sqrt{\pi}$. Substituting this into eq. 12 and integrating gives

$$T_B = \frac{T\alpha_T\sqrt{\pi}}{C}\exp\left[\frac{\alpha_T}{2C}\left(\frac{\alpha_T}{2C}-\sqrt{\pi}\right)\right]. \qquad (13)$$

Eq. 13 is acceptably accurate up to optical depths of 0.7. Antenna smoothing is given by

$$T_A = \varepsilon\int_{-\infty}^{\infty} G(R_P-R_T)\,T_B(R_T)\,\mathrm{d}R_T, \qquad (14)$$

where ε is the transmission efficiency of the antenna system [*Cofield and Stek*, 2006], $G(R_P-R_T)$ is an approximation for the antenna pattern,

$$\begin{aligned} G(R_P-R_T) &= \frac{1}{\mathrm{BW}\sqrt{\pi}}\exp\left[-\frac{(R_P-R_T)^2}{\mathrm{BW}^2}\right], \\ \mathrm{BW} &= \frac{\sqrt{\ln 10 E_t}\,c\,s_T}{\sqrt{5}\,\pi\,\nu\,D}, \end{aligned} \qquad (15)$$

ν is the measurement frequency in GHz, D is the antenna aperture size (160 cm), E_t is the aperture edge taper cutoff (30 db), c is the speed of light (29.979 GHz cm), and s_T is the MLS distance to the limb tangent (3000km). The antenna smearing effect disappears as the width parameter $\mathrm{BW} \longrightarrow 0$. Substituting in eq. 13 into eq. 14, and integrating gives

$$\begin{aligned} T_A &= \frac{\varepsilon T\alpha_T\sqrt{\pi}}{C}\exp\left(\frac{H^2\mathrm{BW}^2a^2}{4T^2}\right) \\ &\times \left[1-\frac{\alpha_T\sqrt{\pi}}{2C}\exp\left(\frac{3H^2a^2\mathrm{BW}^2}{4T^2}\right)\right. \\ &+ \left.\frac{\alpha_T^2}{4C^2}\exp\left(\frac{2H^2a^2\mathrm{BW}^2}{T^2}\right)\right]. \end{aligned} \qquad (16)$$

Some additional approximations are needed to arrive at this result. The exponential in eq. 13 is expanded to first order, the R_T dependence in C is R_p, and the P dependence of α_T is $P_p = \exp[-H(R_T-R_p)]$. Eq. 16 rapidly loses accuracy as BW becomes large because the antenna smoothing includes optically thick radiances where eq. 13 fails. For H_2O near 183 GHz eq. 16 is acceptable for tangent pressures less than 150 hPa. Eq. 16 and 13 show that radiance is linearly proportional to mixing ratio for small α_T. Larger α_T introduces non-linear behavior that reduces $\mathrm{d}T_A/\mathrm{d}f_T$. The limb viewing geometry produces vertically narrow weighting functions; however, according to eq. 8 the horizontal weighting function is a few hundred km. This feature gives MLS high sensitivity to measure low concentrations.

Figure 3 shows scatter plots of H_2O concentration versus radiance for the height and band/channel shown. The radiances were calculated with the full MLS measurement forward model [*Read et al.*, 2006] from a simulated atmosphere without using the approximations in eq. 16. As predicted by eq. 16, all the heights show linear behavior of H_2O mixing ratio with radiance for small concentrations. Also predicted by eq. 16, the higher H_2O concentrations reduce the radiance sensitivity, $\mathrm{d}T_A/\mathrm{d}f_T$, to mixing ratio. This causes the scatter curves to turn-over at higher mixing ratio showing reduced slopes. For 316 hPa H_2O, $\mathrm{d}T_A/\mathrm{d}f_T \approx 0$ at 1000 parts per million volume (ppmv). The H_2O versus radiance curves have non-zero radiance at zero H_2O because the full-up calculation includes dry continuum absorption and other absorbers not considered in the simple theory. These other absorbers cause non-linear radiance behavior with H_2O to occur at a lower concentration than predicted by eq. 16. The dynamic range of H_2O concentrations that can be measured by MLS from 190 GHz (R2) radiometer is 0–1000 ppmv with the limb viewing technique. As $\mathrm{d}T_A/\mathrm{d}f_T$ decreases, the impact of systematic errors on the retrieved H_2O becomes amplified and may be a factor for $H_2O > 200$ ppmv.

The fractional error sensitivity of mixing ratio to other parameters is obtained from differentiating eq. 16,

$$\begin{aligned} \frac{\mathrm{d}f}{f} &= \left(\frac{\mathrm{d}T_A}{T_A}-\frac{\mathrm{d}\varepsilon}{\varepsilon}\right)\frac{1}{\mathrm{X1}}+\frac{\mathrm{d}T}{T}\left(n-\frac{1}{2}-\frac{1}{\mathrm{X1}}+\frac{\mathrm{X2}}{\mathrm{X1}}\right) \\ &- \frac{\mathrm{d}E_t}{E_t}\frac{\mathrm{X2}}{2\mathrm{X1}}-\frac{\mathrm{d}P_p}{P_p}(a+\gamma)-\frac{\mathrm{d}V}{V} \\ &- \frac{\mathrm{d}a}{a}\left(a\ln a+\frac{\mathrm{X2}}{\mathrm{X1}}\right)-\frac{\mathrm{d}\nu_c}{\Delta\nu_c}\frac{\Delta\nu_c}{\nu P^a}\frac{\mathrm{d}\beta}{\mathrm{d}\nu_c}, \end{aligned} \qquad (17)$$

where $\mathrm{d}T_A/T_A$ is the fractional instrument noise, $\mathrm{d}\varepsilon/\varepsilon$ is the fractional antenna transmission uncertainty, $\mathrm{d}T/T$ is the fractional temperature uncertainty, $\mathrm{d}E_t/E_t$ is the fractional antenna edge taper uncertainty (inversely proportional to beam width), $\mathrm{d}P_p/P_p$ is the fractional FOV direction tangent pressure uncertainty, $\mathrm{d}V/V$ is the relative line strength uncertainty, $\mathrm{d}a/a$ is proportional to the fractional line width uncertainty, and $\mathrm{d}\nu_c$ is the channel center frequency uncertainty relative to its bandwidth, $\Delta\nu_c$. The fractional shape factor uncertainty, $\mathrm{d}a/a$ is 0, $-\mathrm{d}w_b/w_b$, $-2P^2w_b^2/\Delta\nu^2/w_b$ for line center, half width, and far wings respectively where w_b is the pressure broadened line width. The functions X1

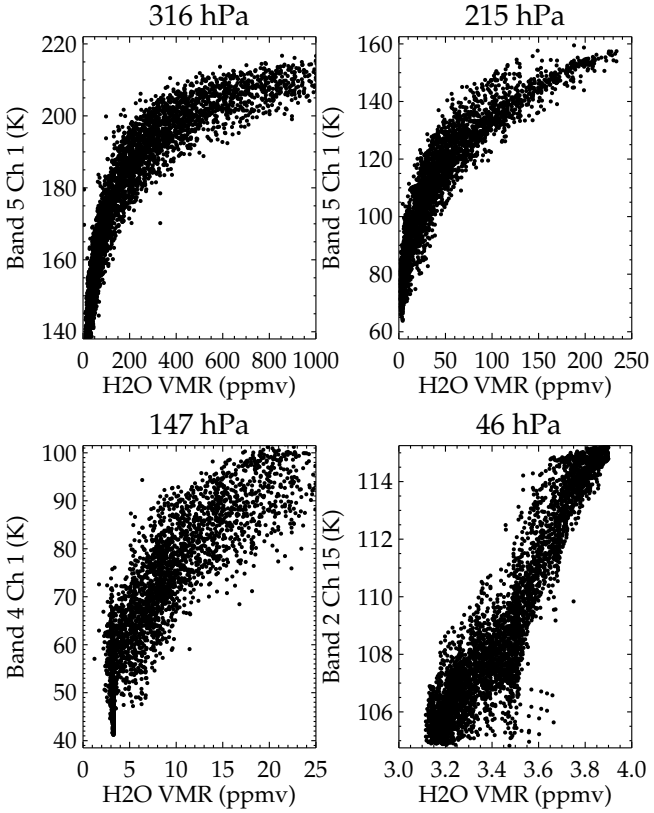

Figure 3. Scatter plots of H_2O mixing ratio versus the given band and channel radiance for the pressure indicated.

and X2 are given below,

$$\begin{aligned} \mathrm{X1} &= 1 - \frac{T'_A}{T_A}\left[\frac{\sqrt{\pi}\alpha_T}{2C}\exp\left(\frac{3H^2a^2\mathrm{BW}^2}{4T^2}\right)\right. \\ &- \left.\frac{\alpha_T^2}{2C^2}\exp\left(\frac{2H^2a^2\mathrm{BW}^2}{T^2}\right)\right], \\ \mathrm{X2} &= \frac{H^2a^2\mathrm{BW}^2}{2T^2}\left\{1 - \frac{T'_A}{T_A}\left[\frac{3\sqrt{\pi}\alpha_T}{2C}\exp\left(\frac{3H^2a^2\mathrm{BW}^2}{4T^2}\right)\right.\right. \\ &- \left.\left.\frac{2\alpha_T^2}{C^2}\exp\left(\frac{2H^2a^2\mathrm{BW}^2}{T^2}\right)\right]\right\}, \end{aligned} \tag{18}$$

where $T'_A = \frac{T\alpha_T\sqrt{\pi}}{C}\exp\left(\frac{H^2\mathrm{BW}^2a^2}{4T^2}\right)$ which is the antenna temperature when $\tau = 1$. Some noteworthy features of eq. 17 are the dependence of radiance errors and transmission on X1 and the approximate cancellation of effects for temperature. A transparent atmosphere has X1 = 1 but becomes zero as the atmosphere becomes opaque. Therefore mixing ratios from optically thick radiances will amplify radiance and transmission errors. This is why for most composition retrievals (tropospheric H_2O being an exception) we avoid using optically thick radiances. The temperature error contribution to mixing ratio show a rough cancellation of absorption n which is usually between 2–3, a hydrostatic term, $-\frac{1}{2}$, and a Planck term $\frac{1}{\mathrm{X1}} \approx 1$. The fourth term is the antenna smearing contribution to the temperature sensitivity. For broad antenna patterns this term is significant. The MLS forward model description [*Read et al.*, 2006] and radiometric calibration [*Jarnot et al.*, 2006] show that uncertainties in the forward model calculation, sideband fractions, calibrated gain, and other calibrated radiance errors behave like an antenna transmission or instrument noise uncertainty. We call this family of errors a radiance scaling error. Unlike the optically thick case, a 1% radiance scaling error for the optically thin radiance causes only a 1% H_2O mixing ratio error. Eq. 18 is used for a few of the systematic error assessments described in appendix A.

References

Cofield, R. E., and P. C. Stek, Design and field-of-view calibration of 114-660 GHz optics of the Earth Observing System Microwave Limb Sounder, *IEEE Transactions on Geosciences and Remote Sensing: The EOS Aura Mission*, *44*, 1166–1181, 2006.

Jarnot, R. F., V. S. Perun, and M. J. Schwartz, Radiometric and spectral performance and calibration of the GHz bands of EOS MLS, *IEEE Transactions on Geosciences and Remote Sensing: The EOS Aura Mission*, *44*, 1131–1143, 2006.

Read, W. G., Z. Shippony, and W. V. Snyder, The clear-sky unpolarized forward model for the EOS Aura microwave

limb sounder (MLS), *IEEE Transactions on Geosciences and Remote Sensing: The EOS Aura Mission*, *44*, 1367–1379, 2006.

Soden, B. J., and F. P. Bretherton, Upper tropospheric relative humidity from the GOES 6.7 μm channel: method and climatology for july 1987, *J. Geophys. Res.*, *98*, 16669–16688, 1993.

This preprint was prepared with AGU's LaTeX macros v5.01, with the extension package 'AGU^{++}' by P. W. Daly, version 1.6b from 1999/08/19.